Interpreting syndepositional sediment remobilization and deformation beneath submarine gravity flows; a kinematic boundary layer approach

Robert W. H. Butler[1]*, Joris T. Eggenhuisen[2], Peter Haughton[3] & William D. McCaffrey[4]

[1] Geology and Petroleum Geology, School of Geosciences, University of Aberdeen, Aberdeen AN24 3UE, UK
[2] Faculty of Geosciences, Utrecht University, PO Box 80.021, 3508 TA Utrecht, The Netherlands
[3] UCD School of Geological Sciences, University College Dublin, Belfield, Dublin 4, Ireland
[4] School of Earth and Environment, University of Leeds, Leeds LS2 9JT, UK
* Correspondence: rob.butler@abdn.ac.uk

Abstract: Turbidite sandstones and related deposits commonly contain deformation structures and remobilized sediment that might have resulted from post-depositional modification such as downslope creep (e.g. slumping) or density-driven loading by overlying deposits. However, we consider that deformation can occur during the passage of turbidity currents that exerted shear stress on their substrates (whether entirely pre-existing strata, sediment deposited by earlier parts of the flow itself or some combination of these). Criteria are outlined here, to avoid confusion with products of other mechanisms (e.g. slumping or later tectonics), which establish the synchronicity between the passage of overriding flows and deformation of their substrates. This underpins a new analytical framework for tracking the relationship between deformation, deposition and the transit of the causal turbidity current, through the concept of kinematic boundary layers. Case study examples are drawn from outcrop (Miocene of New Zealand, and Apennines of Italy) and subsurface examples (Britannia Sandstone, Cretaceous, UK Continental Shelf). Example structures include asymmetric flame structures, convolute lamination, some debritic units and injection complexes, together with slurry and mixed slurry facies. These structures may provide insight into the rheology and dynamics of submarine flows and their substrates, and have implications for the development of sub-surface turbidite reservoirs.

Turbidites and related deposits can contain deformation structures that are interpreted as having formed prior to lithification. Such soft-sediment deformation can include the products of slumping and sliding (e.g. Mulder & Cochonat 1996) or may form by entrainment during dewatering, perhaps triggered by earthquake shaking (e.g. Ross *et al.* 2013; Valente *et al.* 2014). These forms of sediment remobilization can occur on scales from single beds to many kilometres of stratigraphic section. Yet deformation need not imply large-scale instability of the sediment volume, either in response to slope failure or earthquake shaking. Bed-scale deformation can occur during the emplacement of turbidity currents, through shear exerted onto the syndepositional seabed (e.g. Collinson 1994; Clark & Stanbrook 2001; Butler & Tavarnelli 2006; Eggenhuisen *et al.* 2010*a*; McClelland *et al.* 2011; Baas *et al.* 2014). Interpretations of similar deformation have been made for turbulent subaerial gravity flows such as powder snow avalanches (e.g. Sovilla *et al.* 2007) and hot pyroclastic flows (e.g. Sparks *et al.* 1997). Making the appropriate interpretation of soft-sediment deformation is important for establishing the role of different submarine processes. The aim of this paper is to present interpretational strategies for analysing these deformations.

As McClelland *et al.* (2011) pointed out, many synsedimentary structures can be misinterpreted as the products of subsequent tectonics where found in metasedimentary successions within mountain belts. Therefore understanding and recognizing these structures is important to those seeking to unravel orogenic structure. However, these syndepositional structures may also provide clues to the rheology and dynamics of submarine flows and their

substrates during deposition, and their distribution in sandstones within sedimentary basins can affect the performance of hydrocarbon reservoirs.

The paper is organized to introduce a variety of sedimentary deformation structures in turbidites. However, here we lay out criteria for establishing the temporal relationships between deformation and turbidity currents (i.e. subaqueous particulate density currents; in the broad sense, as used by Kneller & Buckee 2000). These then inform a framework for analysing soft-sediment deformation structures, with specific reference to three case studies. Discussion of limitations, alternative interpretations and applications are reserved for the last part of the paper. Some of our examples are familiarly illustrated in textbooks and reviews of sedimentary structures (e.g. Allen 1984). We include these, along with other examples of complex soft-sediment deformation and layer remobilization, to demonstrate that these various structures can all be understood and placed within the context of temporally evolving turbidity currents.

Candidate syndepositional shear structures

A range of structures that might be produced by shear from turbidity currents is illustrated in Figure 1. The bases of many thick turbidite sandstones are characterized by flame structures that inject substrate muds and silt into the bed (Fig. 1a). In some cases these structures are interpreted as the result of loading by the overlying bed (e.g. Kelling & Walton 1957). Thus they are immediately post-depositional. However, it is common to find that the flame structures are asymmetric and are entrained into the overlying
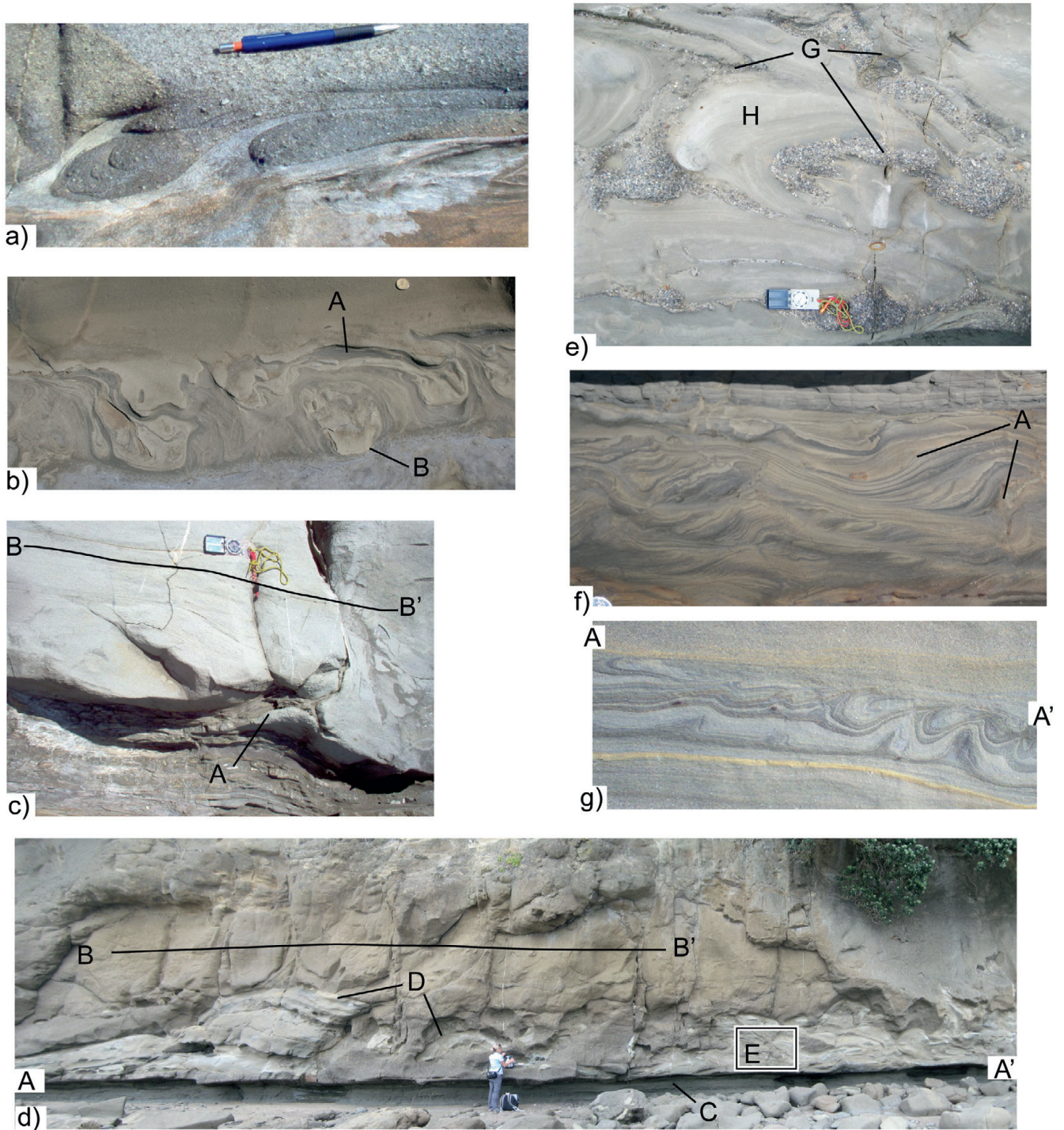
Fig. 1. Candidate examples of structures formed by shear from turbidity currents. In all cases, upper-case letters refer to features within each photograph. (**a**) Strongly asymmetric flame structures where underlying mud- and silt-grade sediment has been injected into a coarse sand at the base of a turbidite sandstone bed. Miocene Macignio Formation, Calafuria, Livorno, Italy. (**b**) Asymmetric, sheared flame structures (A) and foundered sandstone bodies (B) within sheared mudstones beneath a turbidite sandstone. Miocene Waitemata Group; Army Bay, Whangaparaoa peninsula, New Zealand. (**c**) Complex base of a 3 m thick turbidite sandstone bed with wings of sand (A) injected into a substrate of silt-grade sediment. It should be noted that stratification within the main sandstone bed (B–B') is subhorizontal and essentially undeformed, indicating that the complex basal bed structures formed as the sandstone was deposited. Miocene Macignio Formation, Baratti, Piombino, Italy. (**d**) Mingling at the base of a thick gravelly volcaniclastic rudite ('Parnell Grit') with deformed turbidite sandstone substrate. The base of the sandstone (A–A') is interpreted as its original depositional boundary with finer sandstones and siltstones. Above the lower boundary of the rudite, the internal stratification is subplanar and undeformed (e.g. B–B'), indicating that the deformation of its lower interface and intermingling with the turbidite sandstone happened during its deposition. The turbidite sandstone remains attached to its substrate (C) and has been detached into the overlying rudite (D). The location of the detailed photograph is indicated (E). Miocene Waitemata Group, northern Kennedy Beach, Auckland, New Zealand. (**e**) Detail of (**d**) showing complex relationships between injections (seams of gravel: G) derived from emplaced Parnell Grit and folded (H) and sheared former substrate sandstone. (**f**) Climbing ripples and convolute lamination, a classic component of the Bouma Tc interval. Sedimentation within the structures (e.g. A) indicates that folding happened as the fine sandstone was deposited. Miocene Waitemata Group, Little Manley, Whangaparaoa peninsula, New Zealand. (**g**) Amalgamated turbidite sandstone beds with a fold train developed in the lower unit just beneath the common interface (A–A'). Upper Cretaceous Rosario Group, La Jolla Cove, California.

sands. These features imply significant shear strains, the corollary of which is that it is not the vertical loading alone that is important. If the flames have been sheared so too has the surrounding sand. Collectively, the flames and their encasing sand represent a solid-state shear zone. This deformation was presumably imposed either by post-deposition downslope creep or during deposition by the overriding flow. We return to discussing these two mechanisms later. For now we will explore the consequences for this and other deformations resulting from shear imposed by later parts of the same flow that deposited the sand grains.

Flame structures are also a feature of the second example (Fig. 1b). However, parts of the upper sandstone are incorporated, presumably having foundered, into the underlying mudstone. Foundering of turbidity currents into muddy substrates has been re-created experimentally (Baas *et al.* 2014) with the resultant structures reminiscent of these types of sheared outcrop structures. This experimental work illustrates the importance of substrate loading by the flow, rather than necessarily by an aggraded sediment body.

Substrate deformation can include brittle fracture. Eggenhuisen *et al.* (2010*a*; Fig. 1c) described strata-bound fracture arrays developed beneath a 4 m thick sandstone from the Macigno Formation (Miocene, Italy; e.g. Cornamusini *et al.* 2002). This is manifest by wings of the upper sandstone (A in Fig. 1c) penetrating the thinly bedded substrate. Elsewhere along the contact, the substrate has failed by fracture, partially isolating blocks of mud and siltstone. The fractures are filled with sand with the same grain-size population as the base of the overlying sandstone bed. Despite the structural complexity along the base of the sandstone bed, internally its depositional lamination has a simple form. Eggenhuisen *et al.* (2010*a*) interpreted these relationships: the injected sands had been siphoned out of the turbidity current that eventually deposited the sandstone as it passed above, but before it had aggraded the sandstone itself.

More complex substrate interactions include combinations of shear, downward injection and folding. The example here comes from the Waitemata Group (Miocene, New Zealand; e.g. Balance 1974). Here the lower contact between an 8 m thick bed of submarine gravelly volcaniclastic rudite (so-called Parnell Grit; Fig. 1d, showing only the lower 5–6 m of the bed) and deformed turbidite sandstone substrate is considered. The lower 2 m of the rudite bed contains contorted rafts of a sandstone unit that locally retains basal depositional contacts upon further turbidite sandstones, siltstones and mudstones. Deformation in the sandstone rafts involves the overlying rudite. The lower boundary of this deformation coincides with the depositional base of the incorporated sandstone unit (A–A' in Fig. 1d). Gravel-filled seams and contorted bodies are found within the sandstone rafts (Fig. 1e). These can be concordant with the folded lamination of the sandstone and locally discordant (G on Fig. 1e). These relationships are interpreted here as deformed injectites. Folding, injection and refolding indicates a protracted, cyclic deformation history. It should be noted that stratification within the overlying rudite above the complexities of the lower 3 m of the bed (e.g. B–B' in Fig. 1d) is subparallel to the base of the bed base, indicating that deformation had ceased before much of the rudite had been deposited.

All four examples discussed above involve deformation of pre-existing substrate. However, as turbidity currents deposit, sediment derived from the leading parts of the flow becomes the substrate for its more hindward portions. Thus some deformed intervals within turbidite sandstones are bounded by undeformed intervals. Convolute lamination is an example, a classic component of the Bouma Tc interval (e.g. Mutti 1992; Kneller 1995). Here we are concerned with convolute lamination that is asymmetric and shows upwardly varying amplitude (A in Fig. 1f), As McClelland *et al.* (2011) pointed out, these structures formed

during deposition (see Allen 1984) and the shear sense implied by the asymmetry and orientation of folded laminations may be related to palaeoflow determined from conventional sedimentary structures such as flutes, gutters and tool-marks.

The final example (Fig. 1g; from the Rosario Group, La Jolla, California; Hanna 1926) used in this introduction is offered as a candidate for substrate deformation. Here two turbidite sandstone beds are amalgamated, the upper unit having eroded into the underlying one. However, the top of the lower bed is deformed into a train of asymmetric folds. Such structures may be interpreted as having formed by shear transmitted from the turbidity current from which the upper sandstone was deposited but that the deformation happened before the current had evolved to be depositional. Continued passage of the current has eroded the top of the deformed substrate and the deposition that eventually followed caused no further deformation of the substrate. Although such a narrative is consistent with the observations (Fig. 1f), it is not a unique interpretation. An alternative could be that the deformation in the underlying bed entirely preceded the turbidity current from which the upper bed was deposited. In this example it is not possible to establish how much erosion has happened at the interface between the two beds.

Assessing syndepositional deformation

As noted above and in much earlier discussions elsewhere (see Kelling & Walton 1957), the origin of deformation structures found within otherwise undeformed turbidite sequences may be ambiguous. The deformation might be attributed to shear induced by body forces, either by the downslope creep potential of overlying sedimentary deposits (i.e. the bed or beds above the deformed interval) or by the turbidity current that is inferred to have deposited the sediments directly overlying the deformed interval. For our purposes, and to resolve the ambiguity, it is necessary to establish that the specific structures formed contemporaneously with the flow, rather than developed subsequent to it, or possibly even on the ancestral seabed before the overlying bed and its associated flow existed. This problem is equivalent to an exercise in seismic interpretation of kinematic deformation histories of folded or faulted strata: a fundamental issue is to discriminate synkinematic strata from successions that formed before or after deformation. The key for seismic interpretation is to identify 'growth strata' (sometimes described as 'progressive unconformities', e.g. Williams 1993). Here we use the same criteria as for seismic data but, by scaling them down from kilometres to centimetres, apply them to outcrop and well-core.

For illustrative purposes, an example is chosen here from the Eocene–Oligocene Champsaur sandstone of the French Alps, a system described most recently by Vinnels *et al.* (2010). The succession consists of interbedded turbidite sandstones and mudstones that constitute the down-system equivalent of the extensively studied Annot system of SE France (Joseph & Lomas 2004). The studied outcrop (Fig. 2a) lies in high mountain country adjacent to the Col des Pisses (44°43'57"N, 06°19'38"E) with exceptional preservation of bed-scale textures. Palaeoflow regionally was from south to SSE (Vinnels *et al.* 2010). Sparse tool-marks from the base of beds in the studied section accord with this.

Many of the beds in the Col des Pisses section show evidence of minor sediment remobilization, in the form of dewatering pipes, convolute lamination and flame structures. One part of the section is illustrated here (Fig. 2a), centred on a 2 cm thick bed of well-sorted medium sandstone, bounded by mudstones.

The lower interface of the sandstone is flamed and contorted, with local apparent injection of mud from the underlying stratum. The top of the bed is broadly subplanar. There is no evidence that either interface to the sandstone bed acted as a detachment surface.
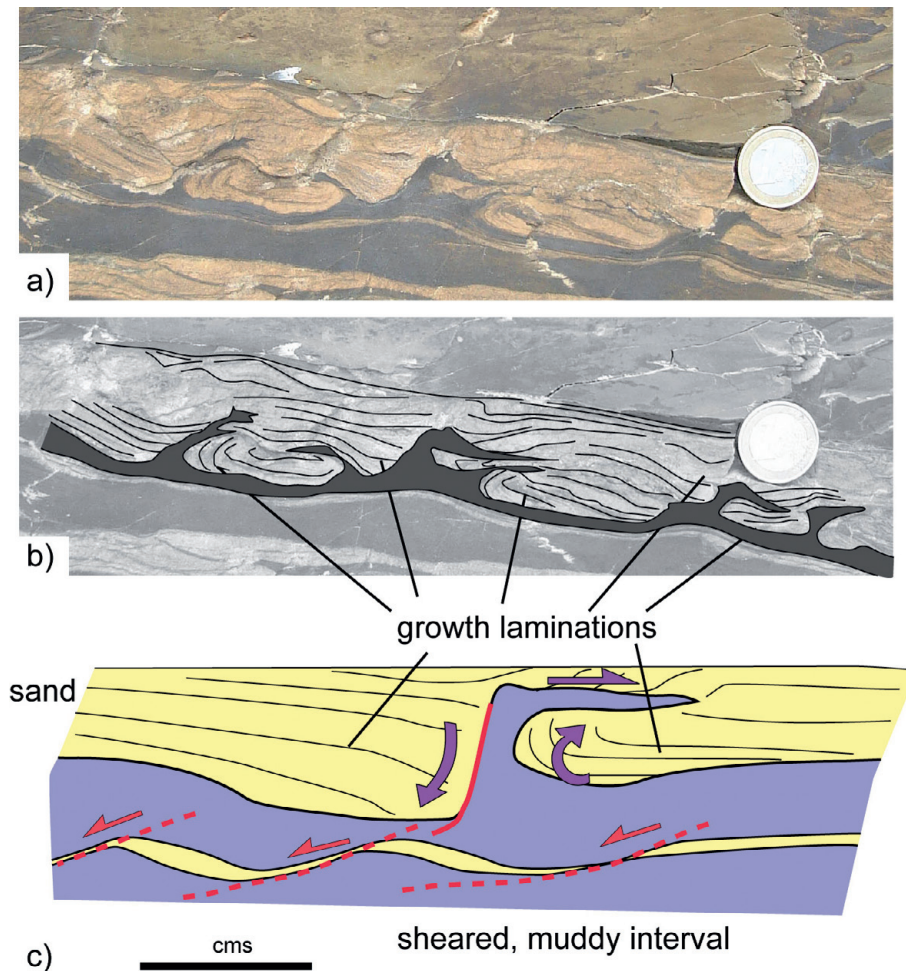
Fig. 2. Example of growth stratification in a bed of fine sandstone above a sheared mud-rich layer; from Eocene–Oligocene Champsaur sandstone of the French Alps (Col des Pisses, Orcières district). Field photograph (coin is *c*. 1.5 cm in diameter. (**a**) uninterpreted; (**b**) interpreted; (**c**) Schematic representation of the stratal and structural geometry imaged in (**a**). It should be noted that deformation in the mudstone interval is coeval with deposition in the overlying sandstone, as charted by depositional lamination (growth strata) in the sandstone.

Consequently, the analysis of deformation and deposition can be restricted to a simple narrative. There are three options for the temporal relationship between the sandstone bed and the deformation of its lower interface: deposition of this sandstone was either before, during or after the deformation.

The deformation of the interface at the base of the sandstone bed demands that the underlying stratum is deformed, whereas the planar upper interface is undeformed. Therefore deformation pre-dated deposition of the overlying mudstone. The key observations are that the depositional laminations within the sandstone also record deformation and that this deformation reduces in intensity (e.g. tightness of folding) systematically moving away from the lower interface of the sandstone bed. This is the classic form of growth strata (Williams 1993); indeed, the form of laminations on this fine bed-scale mimics that imaged at scales 5–6 orders larger on seismic data (e.g. Brun & Fort 2004). Therefore deformation progressed as the sandstone bed was deposited; deposition and deformation were coeval. This elaborates interpretations made of very similar geometries described by Allen (1984, pp. 375–376). Deformation has involved both the original seabed (represented by the lower mud interval) together with deposits left by the overriding turbidity current.

In this example from the Champsaur sandstone, deduction of the relative timing of deformation and deposition is possible because the processes that deposited the sandstone interval formed fine stratification. It is the geometry of this stratification that shows the tell-tale growth patterns diagnostic of synkinematic strata. Such deductions are more complex and uncertain if the growth strata show little or no internal stratification, such as could happen in rapidly deposited beds.

Let us consider the cases of the injectite from the Macigno Formation (Fig. 1b) and intermingled Parnell Grit and Waitemata sediments (Fig. 1c and d). For these examples deformation is most readily interpreted as synchronous with deposition of the overlying bed because in both cases the deformation diminishes gradually away from the lower bed boundary into simple, albeit weak, stratification. If, in either case, the deformation had post-dated deposition of the overlying bed we would expect the entire bed to show the effects of remobilization, not just its lower components. Thus the Macigno sandstone (Fig. 1b) and lower section of the Parnell Grit (Fig. 1c and d), despite not displaying prominent internal lamination, also represent growth strata with respect to the underlying deformation.

The presence of growth strata along the upper interface of a deformed horizon may also be used to infer the likely driving mechanism for the deformation. For the Champsaur example (Fig. 2), there were no beds above the deformed zone at the time of deformation, as indicated by the growth strata, therefore there was nothing apart from the overriding flow to exert shear stresses upon it. Likewise, for the Macigno and Waitemata examples (Fig. 1c and d), little of the overlying bed had been deposited by the time of the deformation and so it cannot have exerted its own body forces into the substrate. The most plausible origin for these deformations is shear stress imposed by the flows that eventually deposited the overlying beds.

A kinematic boundary layer approach

All flows must show a velocity gradient at their base into static substrate. But the submarine flows inferred from the wide variety
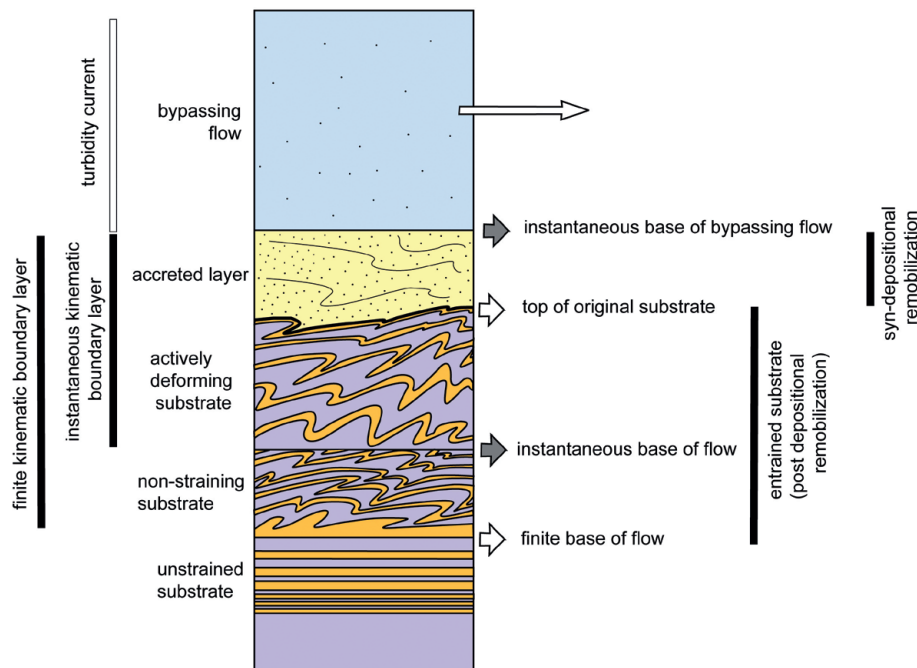
Fig. 3. The structure of kinematic boundary layers formed beneath turbidity currents.

of deposits are widely variable. As Haughton *et al.* (2009) noted, there are several classification schemes for sediment gravity flows, based on sediment concentration, particle cohesion, particle support mechanisms, duration and rheology of the flow. They also noted that some beds produced by single, progressive depositional events can show evidence of being formed by several flow types through time. This implies that single gravity flows can involve different sediment transport processes in space and time; that is, they can be hybrid flows. Regardless of these distinctions we can expect all flows to load and exert shear stresses on their substrate.

The simplest condition applies when a non-depositional (supercritical, in the sense of Kneller 1995; Kneller & Branney 1995) particulate turbidity current runs over a cohesive substrate (Fig. 3). This imaginary current, termed here the 'bypassing flow', will exhibit a displacement gradient at its base, as measured in laboratory experiments (e.g. Cartigny *et al.* 2013; de Leeuw *et al.* in preparation), but will also exert a load that is transmitted into the substrate. The shear stress related to the velocity or displacement gradient at the base of the turbidity current will be equal to the shear stress in the top of the substrate to the flow. For our purposes we are concerned only with that component within the substrate, as, for dilute non-cohesive turbidity currents, the sediment particles remain in suspension and therefore are not, at this stage, part of the geological record. In this paper we are concerned with ancient deposits and thus focus on finite structures and strain that constitute a kinematic boundary layer, formed in response to mechanical loading of the substrate and preserved in the geological record.

As our imaginary turbidity current begins to deposit, sedimentary particles are transferred onto the substrate, and are therefore aggraded onto the kinematic boundary layer. Furthermore, that part of the boundary layer that was deforming could cease, so that the boundary layer could migrate with time through the substrate as the turbidity current continues to pass above, Therefore at a given instant, there can exist an active boundary layer, within which the sediment is deforming, together with an abandoned part of the boundary layer, which has ceased to deform (Fig. 3). In understanding the structural development of these systems it is therefore useful to chart the evolution of boundary layers in relation to the aggradation of the cogenetic deposit. It is an approach

that will be adopted in three case studies below, co-plotting sedimentation and kinematic boundary layer location through (unscaled) time. These plots will then inform further discussions. There are, however, some provisos to this approach.

Although structures preserved beneath and within turbidites may chart the evolution of kinematic boundary layers, intrinsically this record will be incomplete. In common with all deformation, whether strain and structures are developed within the boundary layer will depend not only on the intensity and evolution of these imposed loads but also on the evolving rheology of the substrate. Furthermore, kinematic boundary layer structures may be removed by subsequent parts of the turbidity current through substrate erosion.

A further complication arises when considering systems where the cogenetic turbidity current is not simply dilute and non-cohesive. As long as the overriding turbidity current is non-cohesive, a distinction can be made between the 'bypassing flow', in which all the grains are in significant relative motion, and the cohesive kinematic boundary layer below. Haughton *et al.* (2009) indicated a continuum with increasing particle concentration from non-cohesive to cohesive flows. This transition is enhanced by increasing mud concentrations, thus dampening turbulent suspension mechanisms. Likewise, in high-concentration basal components of turbulent flows, the basal 'traction carpet' (e.g. Mutti 1992) can be considered to form a dilute kinematic boundary layer formed of accreting sediment with rather low shear strength. The approach followed here, and used in the discussion of the Waitemata Group example above (Fig. 1c and d), is to identify the lower deformation boundary within what is otherwise intact substrate and to work up into the composite deposit from below.

The descriptive approach outlined above is now applied to a suite of case studies.

Example 1: normally graded (Tb–Tc) turbidites

Gradually waning turbidity currents are generally believed to create Bouma-type deposits, in which grain size decreases up the bed in parallel with evolving bedforms (e.g. Bouma 1962; Mutti 1992; Kneller 1995). To illustrate this we use part of the Baratti section from the Miocene Magnigno Costieri turbidites of Italy described by Eggenhuisen *et al.* (2010*a*; 43°00'23"N, 10°30'36"E). These
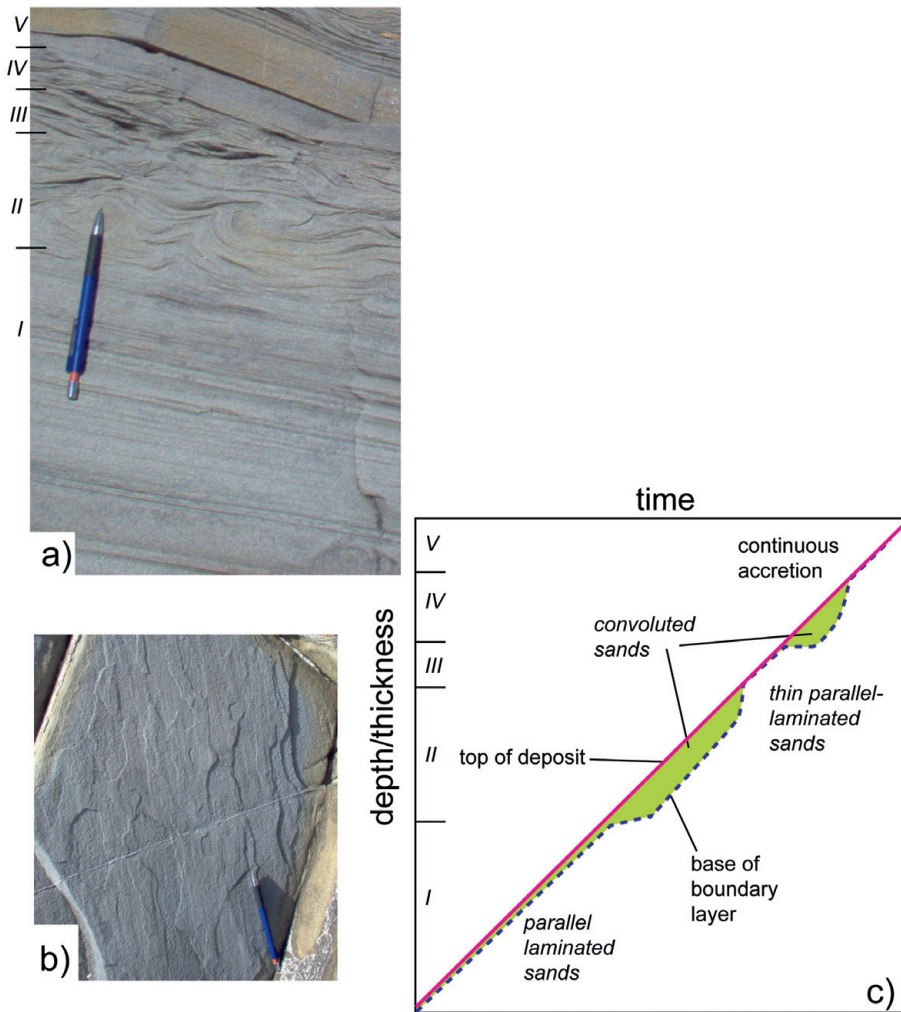
Fig. 4. Kinematic relationships between a turbidity current and its aggrading substrate recorded in Bouma Tb–Tc internals within sandstones of the Oligo-Miocene Macigno Costieri Formation (Cornamusini *et al.* 2002; Eggenhuisen *et al.* 2010*a*) at Baratti (Tuscany coast, Italy). (**a**) View of parallel laminated turbidite sandstone (Tb interval) passing up into convolute lamination (Tc). (**b**) Plan view of planar lamination (Tb interval) with characteristic grain alignment fabric parallel to inferred direction of palaeoflow. (**c**) Unscaled co-plot of deposition and kinematic boundary layer evolution against relative time.

beds (Fig. 4a) consist of parallel-laminated medium-grade sandstones passing up into medium-to-fine sandstones with prominent convolute lamination. These in turn pass up into rippled and sub-planar laminated fine sands or are truncated by the erosional base of the succeeding sandstone.

The planar lamination in the lower interval (I in Fig. 4a) is defined by grain-scale stratification that contains a prominent grain alignment lineation (Fig. 4b). Allen (1984, pp. 259–264) and others subsequently described the alignment process as having formed in the lower boundary layer of the flow. In essence, each lamella represents a kinematic boundary layer to the overriding, and depositing, turbidity current that is just one grain thick. Thus the kinematic boundary layer migrates upwards through the aggrading sediment, lamella by lamella.

The upward transition into convolute lamination (II in Fig. 4a) represents a change in the behaviour of the kinematic boundary layer. This can be tracked by plotting the thickness of the aggraded bed and the base of the kinematic boundary through time (Fig. 4c). The plot is unscaled, simply showing the rate of sediment deposition as constant so that the position of the kinematic boundary layer can be shown relative to sediment aggradation. The co-migration of the top of the deposit and the base of the kinematic boundary layer marks the accumulation of the parallel lamination (I in Fig. 4a and c). Folding involves several depositional lamellae (Fig. 4a) and the kinematic boundary layer involves a greater sediment thickness than for the planar lamination (Fig. 4c). In both of the intervals the kinematic boundary layer evolves through the aggrading sediment. For plane beds the kinematic boundary is simply one grain thick and moves up through the sediment as it aggrades. With convolute lamination the pattern of migration can

be more complex. The precise behaviour can be tracked using the growth strata, back-stripped in the same way as in the analysis of basin-scale folds. Eventually, however, the deformation wanes up section (V in Fig. 4a and c), and is not present in the higher intervals of the bed. Therefore the kinematic boundary layer converges with the syndepositional seabed. For conventional ripples without deformation, the kinematic boundary layer vanishes to have zero thickness as shear is not recorded within the sediment volume.

The change in the kinematic response to shear beneath the turbidity current between the planar to convolute lamination intervals could reflect: a change in the mechanics of the overriding, bypassing flow, such that it transmitted a higher shear stress into the substrate; or evolution of the rheology of the sediment beneath the flow; or a combination of these. As convolute lamination is a common feature of turbidite sandstones of fine sand-grade, of the options above it seems most likely that the behaviour signifies a change in substrate rheology. As Kneller & Branney (1995) discussed, the combination of rate of deposition and grain-size distribution decreases the permeability of the accreting layer to a point where not all the excess pore-water can be diffused through the compacting bed. This would allow the effective normal stresses on grain contacts within the bed to remain low enough so that thresholds of static friction are easily overcome as long as the conditions last (e.g. until the rate of deposition slows down).

Example 2: substrate disaggregation, entrainment and shear

As discussed in the introduction, many candidate syn-emplacement shear structures are found beneath turbidite sandstones. An
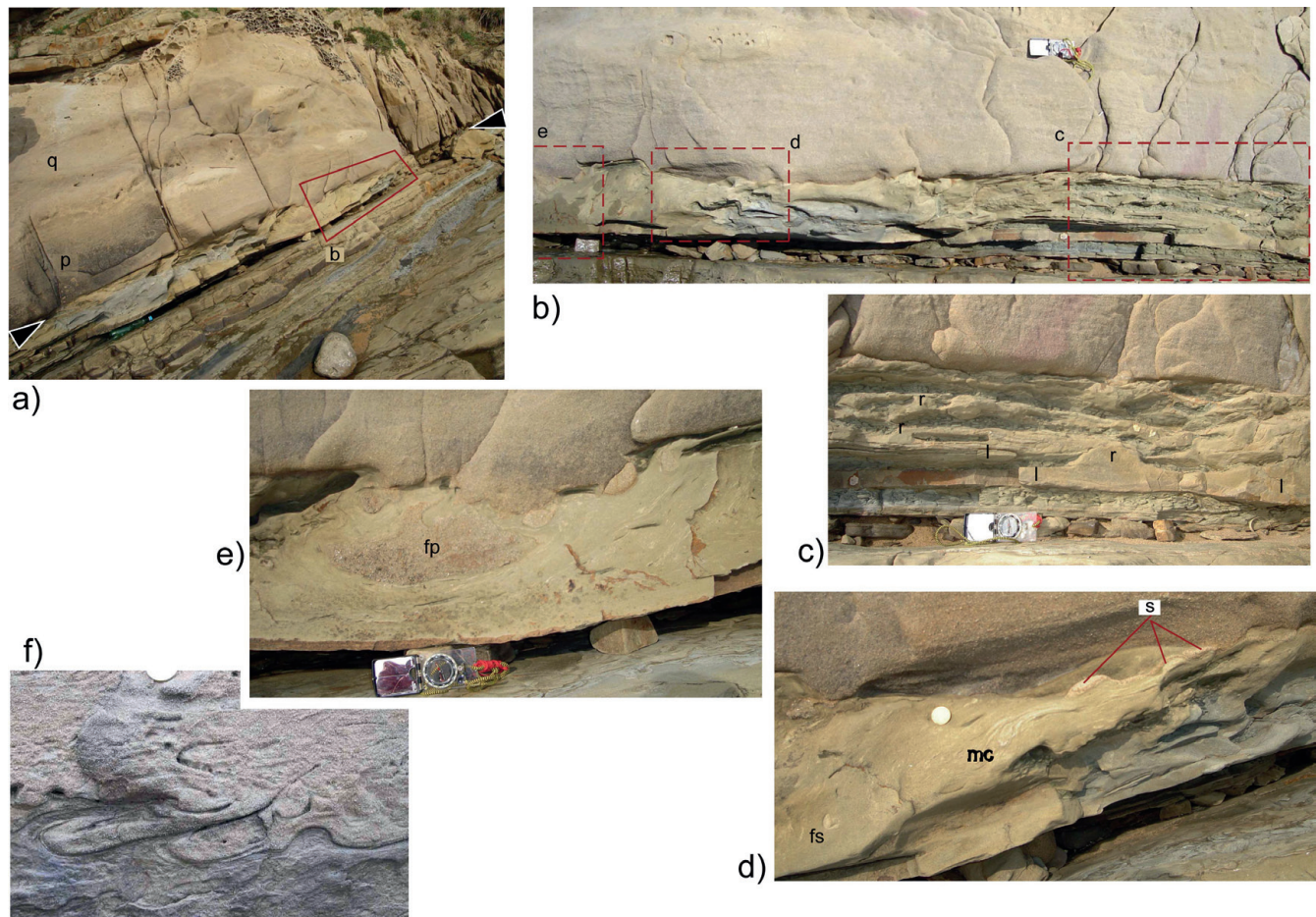
Fig. 5. Substrate–turbidite relationships recorded in outcrops of the Miocene Policca Formation (Amore *et al.* 1988; Cavuoto *et al.* 2004), Cilento, Italy. These outcrops lie at the northern end of the Lago Santa Maria bay. (**a**) View of outcrop with the base of the 4 m thick bed of interest arrowed, with deformed substrate derived from the thin-bedded units below. The detailed area of this boundary layer is the boxed area (**b**). The coarsely banded lower part of the bed of interest (p) and the dewatered interval characterized by dish and pillar structures (q) are indicated. The bed top is not visible in the photograph. (**b**) Panel of the base of the bed of interest with distinct portions of the substrate identified for following detailed photographs. In this and other photographs the open compass is 17 cm across. The coin is *c*. 2.5 cm (**d**, **f**) in diameter. (**c**) Largely intact thin-bedded fine sandstone–mudstone couplets. The fine sandstones generally preserve depositional contacts with the adjacent mudrocks together with primary depositional lamination (l). However, in places these sands are remobilized (r) and cross-cut the mudstones to form a branching sandstone web. (**d**) Here the substrate consists of a debritic muddy fine sandstone with sheared mudstone clasts (mc) and thin stringers of fine sandstone (fs). This facies is interpreted as an essentially *in situ* disaggregated mixture of the substrate units shown in (**c**). Stringers of coarse sandstone (s), interpreted to have been incorporated from the turbidity current that deposited the overlying bed, are infolded with the muddy–sandy debrite. (**e**) Pendants of coarse sandstone (fp) foundered into the muddy–sandy debrite. (**f**) Folded and flamed interface at the base of the coarse bed of interest, *c*. 2 m right of view in (**a**).

example presented here comes from the Miocene Policca Formation of the Cilento district of Italy (Amore *et al.* 1988; Cavuoto *et al.* 2004). This forms part of a mini-basin fill developed above thrust sheets in the southern Apennine orogeny. Sandstone event beds in the Lago Santa Maria section (40°18'49"N, 14°56'40"E) can attain thickness of 5 m, although the unit (Fig. 5a) discussed here is *c*. 4 m thick. The lower interval of this bed is coarse sand-grade with bed-parallel, subplanar stratification that broadly fines up into medium–fine sand with a silty–muddy cap. This bed overlies centimetre-thick fine-grained laminated turbidite sandstone and silty mudstone couplets (Fig. 5a). The different grain-size fractions are useful as tracers, distinguishing within the boundary zone material that originated within the turbidity current from which the upper bed was deposited from that derived from its substrate.

A 6 m lateral section of the base of the coarse sandstone bed is exposed, which shows significant structural heterogeneity (Fig. 5b). In places the contact with substrate is abrupt and bed-parallel to intact substrate beds that contain primary depositional stratification. Elsewhere the substrate is represented by a debrite of silty mudstone blocks in a branching network of fine sandstone

(Fig. 5c). At other locations along the contact, the substrate is formed by a poorly sorted mixture of silt and fine sand with small, distorted fragments of silty mudstone clasts (Fig. 5d). All these different substrate forms show transitional relationships with one another (Fig. 5b) interpreted here as representing different states of disruption and disaggregation. Thus the mixed silt and fine sand facies is interpreted as forming from disaggregation and mixing of the fine sandstone and silty mudstone. The outcrop preserves the lateral transition between these two facies. An intermediate position contains a branching sandstone form within which the primary depositional lamination in the sandstone is lost. These relationships are interpreted as representing disaggregation through liquefaction of the sandstone. At low states of disruption the remobilization product is a silty mudstone breccia with clasts that are barely misoriented with respect to the intact substrate stratigraphy. Further fluidization of the silty mudstone allowed mixing of this material with the adjacent fine sand.

The mixed silt and fine sandstone material contains stringers of coarse sand, some of which can be traced up to the overlying coarse sandstone bed (S in Fig. 5d). This indicates that the deformation and shearing within the mixed silt happened as the flow
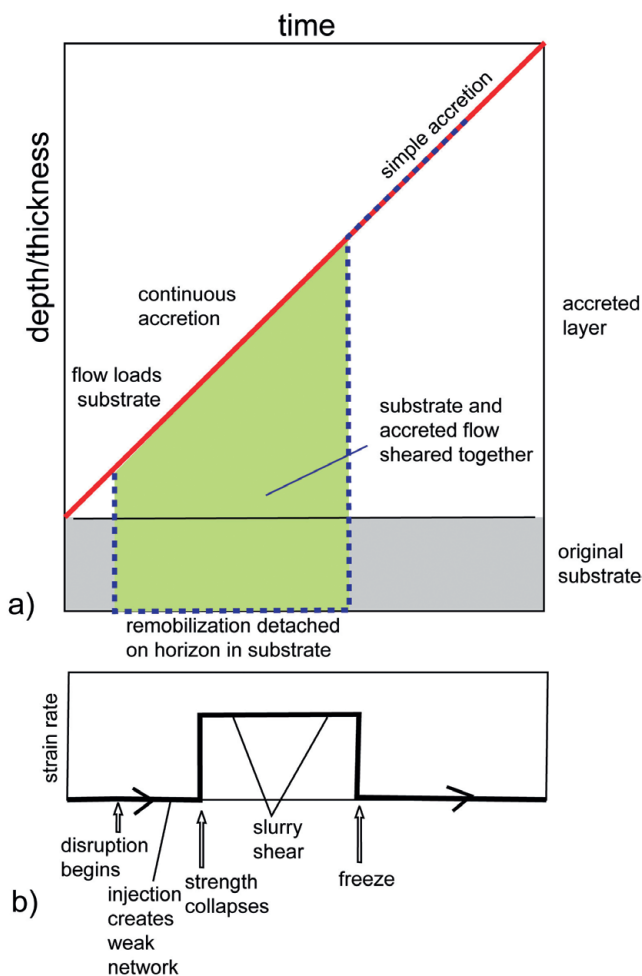
Fig. 6. Interpreted evolution of the kinematic boundary layer shown in Figure 5. It should be noted that this history varies along the base of the bed of interest. (**a**) illustrates the involvement of substrate into a kinematic boundary after a small amount of deposition of the overriding turbidity current. Eventually deformation ceases and deposition of the main bed continues. (**b**) relates this evolution to strain rate, with catastrophic strength collapse as the substrate disaggregates into a muddy–sandy mixture. This disaggregation starts after some low-strain deformation in the substrate (local liquefaction and injection of sand). However, the end of the substrate deformation coincides with a radical reduction in the thickness of the mechanical boundary layer, as deposition continues.

that deposited the thick, overlying sandstone bed was being emplaced. Foundered balls and pendants of coarse sand also lie at the interface between the mixed silt–sandstone unit and the overlying turbidite bed (Fig. 5c). Within a few centimetres up into the upper thick overlying sandstone bed, its internal stratification is simple and subplanar, indicating that the interfacial mixing happened prior to aggradation of all but the lowest portion of the upper bed. Further corroboration that deposition and substrate remobilization are contemporaneous comes from further along the interface, where an inverted mushroom-shaped pendant of coarse-grained sandstone (fp in Fig. 5e) is encased in silty sandstone. This is readily interpreted as a foundered mass of newly deposited sand from the turbidity current. It is overlain by laminated turbidite sandstone, indicating that the foundering happened as the overlying bed aggraded. Similar foundered masses of turbidite sandstone, displaying internal growth laminations (Fig. 5f) similar to those seen in the Champsaur sandstone example (Fig. 2), also testify to the syndepositional nature of the deformation along the lower interface of the turbidite.

Disaggregation processes within the substrate to turbidites, like those described above, were invoked by Butler & Tavarnelli (2006) to explain remobilization of metre-thick turbidite sandstones beneath a 20 m thick sandstone unit in the Miocene Gorgoglione 'flysch' of the southern Apennines of Italy. A plausible mechanism for substrate liquefaction is the loading, enhanced by high-frequency reverberations caused by turbulence within the overriding turbidity current (Røe & Hermansen 2006). If so, deformation of the substrate can begin after some passage of the turbidity current. As deformation incorporates the lowermost portion of the overlying turbidite we deduce that deposition had begun from the flow as the substrate deformed (Fig. 6). We further infer that the mixed silty–sand unit was weaker than the original, intact substrate and so it is into this unit that the overlying coarse sand has preferentially been incorporated. Eventually, however, deformation in the substrate ends, freezing in the structures preserved in outcrop. The cessation of deformation could relate to work-hardening of the substrate, perhaps linked to draining of pore fluid into the overriding turbidity current together with armouring of the weak substrate by coarse sand deposited by the turbidity current. That this current continued to pass over the now-deformed but stable substrate is indicated by the deposition of undeformed, stratified coarse sand above the bed base. Had deformation continued we expect the higher parts of the coarse sandstone bed to be deformed with the substrate.

Deformation and dewatering of the sandstones in the Lago Santa Maria section that hosts this example have recently been used to infer synsedimentary seismic activity (Valente *et al.* 2014). We suggest that such causal relationships be treated with caution given the protracted syndepositional shearing described above.

Example 3: slurry facies in the Britannia sandstone

Syndeposition shear fabrics are a component of so-called 'slurry facies' in sandstones presumed to be deposited from high-density turbidity currents (Lowe & Guy 2000). The type example for this facies is found within the Lower Cretaceous Britannia Sandstone (UK Continental Shelf). A characteristic of many Britannia Sandstone sections, especially from upper reservoir levels, is the development of centimetre-scale light and dark band couplets. The tonal variations reflect slightly higher clay content in the dark bands. The dark bands generally show shear structures picked out by deflected and attenuated wispy dewatering pipes and sheets. The light bands in contrast show grain-scale depositional lamination. It is these couplets of light and dark bands, and alternating deformation, that characterize the slurry facies. Lowe & Guy (2000), Lowe *et al.* (2003), Barker *et al.* (2008) and Haughton *et al.* (2009) interpreted these intervals as recording transient periods of cohesive flow in the lower part of the turbidity current that deposited the thick sandstones. The shear fabrics are evidence for cohesive flow, formed synchronously with the deposition of the muddier interval in each couplet: layer composition and structure are genetically related. Migrating sand–mud-rich sediment couplets have been created experimentally by Baas *et al.* (2011) with suspended sediment concentrations of 8%. They did not, however, create shear fabrics in the muddier unit that is seen in the equivalent banded interval in the Britannia Sandstone. The kinematic approaches in the current paper challenge this and we offer an alternative interpretation, as can be illustrated using a single type-example.

Bed 78 (Barker *et al.* 2008) in the upper Britannia reservoir is up to 11 m thick (Fig. 7a) with a systematic grain-size structure indicative of deposition in a single continuous, albeit sustained, event (Barker *et al.* 2008). Here we examine the middle part of this
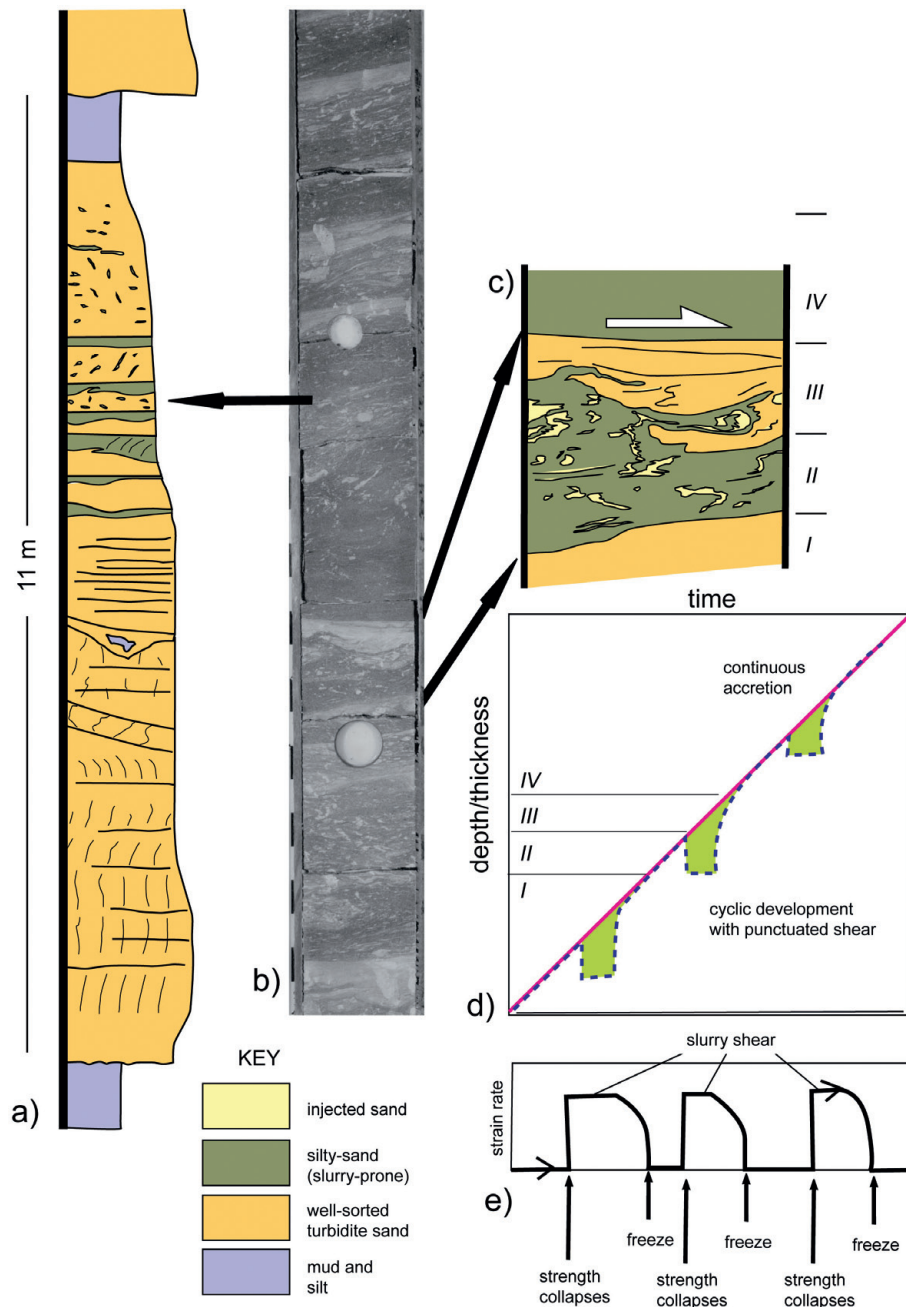
Fig. 7. Banded 'slurry' facies from the Britannia Sandstone (Bed 78 of Barker *et al.* 2008; well Chevron 16/26-B1). (**a**) Simplified log for Bed 78. (**b**) Representative core stick for the banded 'slurry' facies located on the sedimentary log. The characteristic tonal banding enhances minor variations in clay content (greater in the darker bands). Pale streaks in the darker bands are shared dewatering pipelets and sheets that formed during the shear. Deformation along the lower interface of the pale bands is also charted by internal depositional lamination, indicating that deformation in the darker bands happened as the pale bands were deposited. The width of the core stick is 10 cm. (**c**) Interpreted sketch of a banded couplet. (**d**) Unscaled co-plot of deposition and kinematic boundary layer location v. time. Depositional and deformation cycles migrate, albeit at different rates, upwards with time. (**e**) displays this behaviour in terms of strain rate cycling through time (in phase with (**d**).

bed, where the banded slurry facies is found (Fig. 7b). This has the characteristic couplets of pale and dark bands. Well-developed shear structures, picked out by deflected, contorted and attenuated dewatering streaks, are developed in the dark bands. The pale bands (fine sandstone) preserve grain-scale depositional lamination. The lower interfaces of the pale bands are commonly undulated and locally involved in strongly asymmetric flame structures (Fig. 7c). The lamination within the pale intervals shows synkinematic growth patterns, equivalent to those illustrated in Figure 2.

The observations and first-order interpretation outlined above suggest a complex cycling between deposition and deformation, shown schematically in Figure 7d, and referenced to a single couplet (Fig. 7c). The deposition of unit II was followed by dewatering, presumably sourced from the just-deposited underlying parts of Bed 78, as marked by thin pipes and sheets. These are deformed, indicating that the kinematic boundary layer stepped down into layer II, but not as deep as layer I. The kinematic boundary continued to deform as the pale band (III) was deposited but eventually stepped up out of this unit so that the upper parts are undeformed

(IV). Each couplet presumably reflects this cyclic behaviour, thus building up a succession that shows layer-confined deformation, corresponding to the bands.

The evolution of the kinematic boundary layer through a package of banded slurry facies couplets can be charted qualitatively in terms of the strain rate within the aggrading bed (Fig. 7e).

The key insight from the approach adopted here is to identify that the shear fabrics in the slurry couplets were formed while the cleaner sandy interval deposited, and not necessarily the clay-richer interval. It is the sedimentology of this capped sandy unit that gives insight into the processes that generated shear strains in the substrate that in turn operated near-bed in the coeval turbidity current. The shear structures do not relate to the deposition of the levels that contain them (see Lowe & Guy 2000, and subsequent work) and therefore cannot be used to infer the rheology of the part of the flow from which the dark intervals were deposited. The pale bands, which have good grain-size sorting, record the dynamics of that part of the turbidity current that was shearing its substrate.
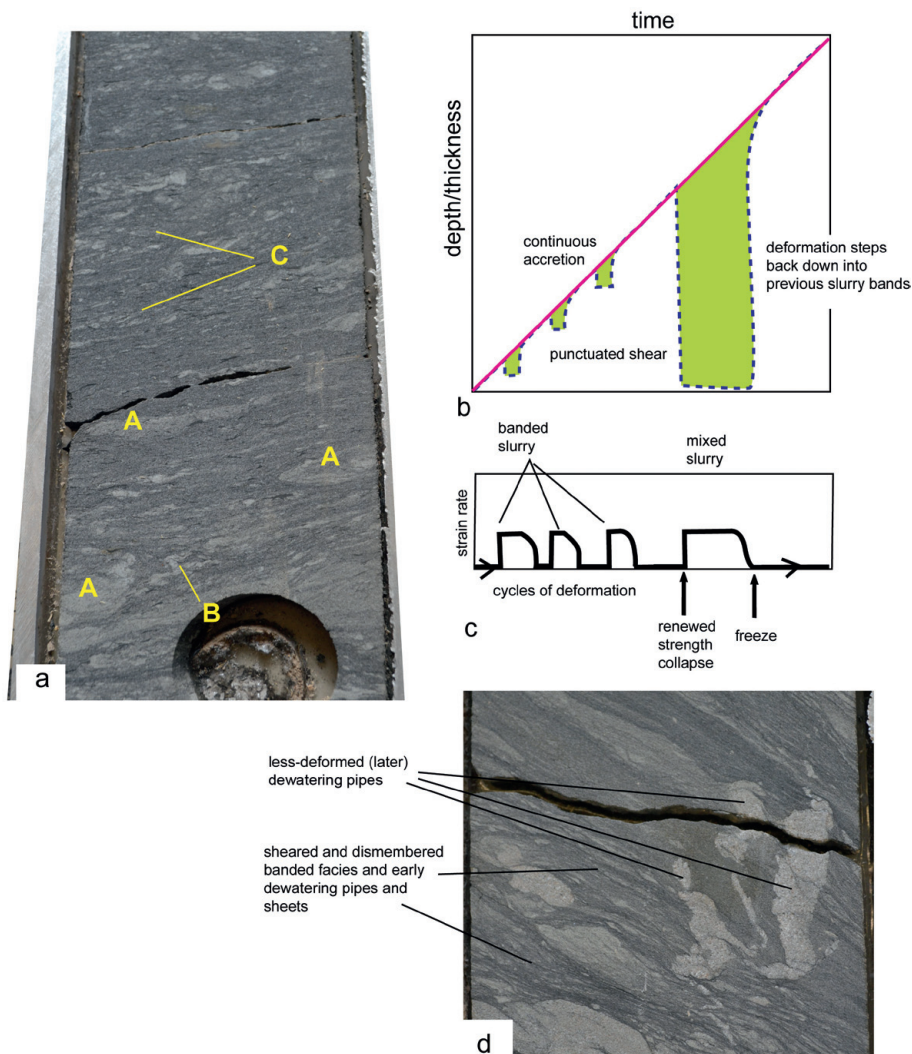
Fig. 8. Typical 'mixed slurry' facies from the Britannia Sandstone. (**a**) Core photograph (Chevron 16/26-B3; width of core is 10 cm). Example textural elements: A, folded lens of laminated fine sandstone (disrupted pale band); B, sheared streaky dewatering pipelet; C, shear fabrics. (**b**) Unscaled co-plot of deposition and kinematic boundary location v. time. The initial evolution, forming a tied stack of banded slurry facies, is as in Figure 7. However, the mixed slurry develops by a remigration of the kinematic boundary down into previously sheared sediment, creating polyphase shear structures. (**c**) Hypothetical strain rate plot showing cycling deformation as the kinematic boundary layer evolves (in phase with (**b**)). (**d**) Typical relationships between variably deformed and dismembered banded (slurry) facies, early formed (and strongly attenuated) dewatering pipes and later (less deformed) pipes, indicating that the deforming material was recharged with water during deformation.

Mixed slurry facies

Bed-confined shear fabrics within the Britannia Sandstone are not restricted to the centimetre scale as discussed so far. The 'mixed slurry facies' of Lowe *et al.* (2003) can involve bed thicknesses >1 m. Those researchers identified that these mixed slurries contain disrupted light bands (Fig. 8a), indicating a two-stage formation that reworks the banded slurry facies described above. Lowe *et al.* (2003) and Eggenhuisen *et al.* (2010*b*) suggested that the reworking of the banded slurry facies happened by post-depositional creep rather than processes associated with turbidity current activity. This original interpretation cannot be ruled out, largely because of the scale of remobilization and the limitations of well-core in constraining lateral variations in bed structure. Unlike the 'slurry' facies (Fig. 7), it is difficult to identify clear growth strata associated with deformation in 'mixed slurry'. Therefore, deductions about the timing of the deformation relative to turbidity currents remain ambiguous. However, the 'mixed slurry' facies are commonly sandwiched between intervals within single event beds that are not disrupted. Thus it is possible that the reworked facies developed during bed aggradation and thus relate to processes intrinsic to the depositing flows rather than an additional mechanism. That these fabrics developed during the deposition of the event beds is further indicated by the fabrics deforming but also being cross-cut by dewatering stringers and pipes that elsewhere can be inferred to develop during bed aggradation (Fig. 8d).

Kinematic boundary layer processes can explain the development of 'mixed slurry' facies (Fig. 8a), through the multi-stage evolution outlined above. Once a few couplets of the centimetre-scale banded slurry facies have been deposited the kinematic boundary could step down deeper into the substrate (Fig. 8b) to rework the earlier, aggraded sediments. As with the slurry facies, this behaviour implies cycling of strain rate in the substrate of the evolving turbidity current (Fig. 8c). This interpretation raises issues with the rheological evolution of the deposit. Intuitively, we might consider deformation such as described here to be work-hardening, as pore fluid is expelled by shearing. However, as porosity is lost the permeability of the actively deforming kinematic boundary layer may also reduce, acting to trap or inhibit fluid escape from lower in the host bed. This in turn could serve to re-weaken the deposit, leading to a second failure event and the down-cutting of the kinematic boundary layer into previously deformed sediment. That dewatering of underlying layers progresses during shearing, charging the kinematic boundary layer, is indicated by cross-cutting arrays of fluidization pipes and sheets at differing states of deformation (Fig. 8d).

Discussion

Kinematic boundary layers and their spatial–temporal location

The deformation structures examined in the case histories record the evolution of kinematic boundary layers at different stages during the passage of their causal turbidity currents. Turbidity currents can evolve show significant variations in internal organization along their length (e.g. Postma *et al.* 2009), with highly energetic, turbulent heads, vertically stratified flow behaviour with a higher-concen-
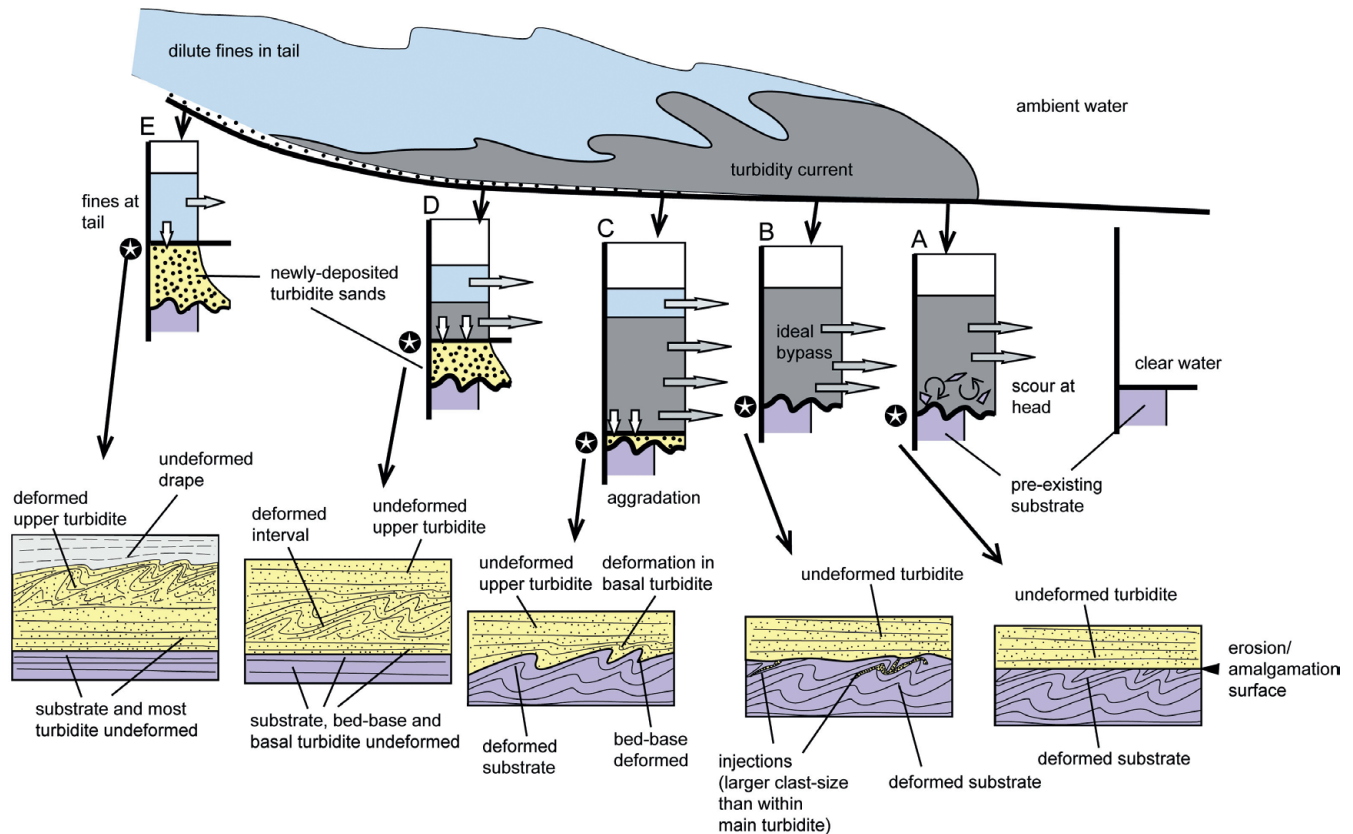
Fig. 9. Summary of locations and timing of deformation beneath an idealized turbidity current. If the head of the flow is erosive (A), any substrate deformation structures are prone to decapitation and sands deposited by subsequent parts of the flow will aggrade across these structures (e.g. Fig. 1g). Behind the head (B), but prior to significant deposition from the flow, deformation of the substrate can incorporate sediment from the turbidity current, siphoned into fractures and preserved as injections (e.g. Fig. 1c). Should deformation of the substrate happen as sediment is being deposited (C), the substrate, lower part of the overlying bed and their common interface will be deformed (e.g. Fig. 5). Deformation might begin after some sediment has been deposited from the turbidity current (D), creating strata-bound deformed intervals within the aggraded bed (e.g. Fig. 7). Finally, deformation might happen towards the rear of the turbidity current (E), represented by sheared bed-tops draped by siltstones (e.g. Fig. 1f). Some or all of these relationships between deformation and deposition can happen at the same site during the passage of a single turbidity current, creating tiered deformation through a turbidite sandstone and its immediate substrate.

tration, potentially slower-moving lower layer, and a dilute tail. These different domains are likely to exert different loads on their substrates, and these behaviours are also likely to vary in response to variations in the incidence of the current with pre-existing variations in seabed morphology. During the passage of a turbidity current, different parts of the seabed will have different initial and evolving rheologies so that the substrate response can vary in space and time. Furthermore, the capacity of the flow to transport sediment will vary in time and space so that more hindward portions of flows can pass over substrate that includes sediment deposited from the more forward portions. These substantial heterogeneities promote the variety of kinematic structures discussed here. However, some simple relationships allow these structures to be placed in the context of the turbidity current that formed them (Fig. 9).

Where flows are essentially bypassing before any deposition, any deformation of the substrate can be prone to erosion. This can leave a kinematic boundary layer that has no temporal relationship to its overlying deposit (situation A in Fig. 9), which aggraded from the turbidity current after it had ceased shearing its substrate. In these situations, relating deformed intervals to overlying beds is uncertain; indeed, the deformation might relate to an unrecorded flow that left no deposits, or these deposits may have been eroded by the flow that eventually deposited the overlying bed. In some outcrop situations it may be possible to discriminate between these scenarios by establishing if the erosional surface above the deformed interval records the passage of multiple flows; for example, by identifying multi-generation populations of tool-marks and

scours upon it. However, if the deformation involved brittle failure then the flow to which the structures formed a kinematic boundary layer may have been sampled in sand injections (situation B in Fig. 9). These may be preserved even though the rest of the flow at that time was bypassing this part of the seabed.

Less ambiguous relationships, charted by growth strata, will be found at locations on the seabed that are accumulating sediment from the turbidity current as it shears its substrate (situation C in Fig. 9) or its just-aggraded deposit alone (D in Fig. 9). Therefore kinematic boundary layers will be most readily interpreted for flows that are in active phases of deposition. However, as with the relationships created towards the head of a bypassing flow, the hindward regions may also generate ambiguous relationships. Deformation recorded by bed-tops, in the absence of growth strata, could have been caused by post-depositional processes.

Kinematic boundary layers and flow dynamics

The analysis of kinematic boundary layers may yield valuable information on the dynamics of turbidity currents. The processes described here might be viewed as precursors to erosion, especially where the deformation products are weaker than the original substrate. Presumably, many kinematic boundary layers are lost through erosion, especially when developed by the heads of turbidity currents. It remains unclear how the distribution of kinematic boundary layers might relate to seabed configurations such as down-transport gradient changes or to any lateral restrictions.

There is the possibility that mapping the patterns of syndepositional deformation, together with well-established methods such as comparing palaeoflow indicators between the tops and base of beds (e.g. Kneller *et al.* 1991), could yield valuable information on the geometry of ancient sedimentary basins. There are parallels with structures described from ignimbrites, the depositional products of subaerial particulate gravity flows (e.g. Branney & Kokelaar 1992), where various sheared textures have been used to infer how the causal pyroclastic flow evolved rheologically.

Substrate deformation can feed back into the dynamics of the overriding flow as it perturbs the geometry and rheology at the base of the flow. Eggenhuisen *et al.* (2010*a*) noted that dune-like bed morphologies developed above steps created by injections isolating substrate blocks in the Macigno sandstones (Fig. 1c). Fluid mud substrates may affect the lower boundary interactions of gentle flows by effectively dampening turbulence (e.g. Verhagen *et al.* 2013).

Flows other than turbidity currents can develop deformation structures in their substrates, creating structures similar to those described here. Matsumoto *et al.* (2008) described asymmetric flame structures that have formed and been truncated, then buried in further sedimentation during the aggradation of a tsunami deposit.

The coexistence of turbidite sandstones and sheared, muddier rocks is commonly interpreted as the result of competing long-transport flow processes in submarine density currents (e.g. Haughton *et al.* 2009; Talling *et al.* 2012). The interpretations here offer alternative explanations that may be appropriate for some examples elsewhere in the literature. A key deduction, reached here in consideration of the Britannia Formation, is that the deformation structures found in the sediments do not, of themselves, relate to the dynamics of the turbidity current that induced that deformation. All deformations recorded here require the sediment, at the time of this deformation, to be in grain-to-grain contact and for this to have been maintained subsequently. Clearly then, the structures relate to 'laminar' or some other non-turbulent flow processes. The turbidity current that exerted the shear stress that drove these deformations could have a variety of flow mechanisms, including entirely turbulent processes. The processes acting within the turbidity current at the time of deformation of its substrate are recorded, at least in part, by the growth strata.

An additional complexity in attempting to deduce the dynamics of turbidity currents from the structural evolution of kinematic boundary layers is that deformation need not simply migrate upwards through a deposit with time, in an approximation of the law of superimposition. If our interpretation of the mixed slurry facies from the Britannia Formation (Fig. 8) is correct, deformation can cut deeper into an aggraded sediment pile with time. It may therefore be difficult to relate the structures to particular processes active at times in the history of a causal turbidity current.

Implications for palaeoflow

In their study of convolute lamination, McClelland *et al.* (2011) presented convincing evidence to relate the vergence of folds to palaeoflow recorded by the host turbidite. Similarly, Butler & Tavarnelli (2006) showed how small-scale structures found beneath a thick turbidite sandstone relate to erosional palaeoflow indicators at the base of this sandstone. Both are examples of what we have here termed kinematic boundary layers. In effect, these boundary layers are shear zones and therefore should yield a range of asymmetric shear criteria similar to those that are used to determine kinematics in metamorphic shear zones (e.g. Hanmer & Passchier 1991). However, natural shear zones, especially where the deformation is not ideal simple shear, can yield ambiguous relationships. Heterogeneous strain partitions can create local reversed shear senses. Furthermore, the deformation in kinematic boundary layers is unlikely to have been constant volume, as it will

be accompanied by changes in pore volumes. Differential compaction effects, including those developed post-kinematically, can enhance and locally reverse apparent shear senses. Further research is needed to establish if systematic shear senses can be related to palaeoflow in kinematic boundary layers.

Alternative explanations and potential misinterpretations

The strong resemblance of shear fabrics within intervals such as in the mixed slurry facies (Fig. 8) to s–c and shear band development in mylonites (e.g. Hanmer & Passchier 1991) could lead to confusion when studying turbidite sections in orogenic belts. Likewise, convolute lamination is open to confusion with tectonic deformation structures (as noted by McClelland *et al.* 2011). Identification of growth strata with these structures removes the ambiguity.

We do not wish to imply that all soft-sediment deformation need represent kinematic boundary layers for turbidity currents. Post-depositional processes, such as downslope creep, are clearly important, such as has been described for hot pyroclastic flows (e.g. Kobberger & Schmincke 1999). The key feature of the kinematic boundary layer model described is the requirement that deformation happened at the same time as the structures were being overridden by a turbidity current. Yet simply demonstrating a temporal relationship between deformation and deposition does not, on its own, require a causal relationship. However, repeated cyclic development of deformation during aggradation of a single bed (e.g. the slurry facies in the Britannia Sandstone Formation, Fig. 7), or repeated development of deformation in the equivalent intervals of a series of beds (e.g. convolute lamination, Fig. 4), is more plausibly related to intrinsic flow–substrate interactions, rather than responses to external forces such as earthquakes.

Implications for subsurface reservoirs

The Britannia Sandstone Formation that provided the examples of 'slurry' textures here (Figs 7 and 8) hosts a major gas condensate field. The lateral equivalent Captain Sandstone Formation, part of the turbidite sand fairway in the Moray (e.g. Pinnock & Clitheroe 1997), is a target for subsurface carbon storage (Garnham & Tucker 2012). The subsurface petrophysical properties of these and other turbidite sandstones around the world are important in their exploitation as subsurface reservoirs. So too is the architecture and distribution of heterogeneities within these formations. Deformation in poorly lithified sandstones repacks the grains and consequently can change both the porosity and permeability in deformed strata (e.g. Fossen *et al.* 2007). Sand injections developed within kinematic boundary layers (e.g. Fig. 1c) can enhance vertical connectivity between sandstone units. Contrasting interpretations of textures (for example, as representative of kinematic boundary layers as distinct from, for example, debris flows) are likely to have different predictions of the distribution of these textures through basins. As mentioned above, further research is needed to establish how different configurations of flows and sea-floor morphology can affect kinematic boundary layer development. Until then, predicting the distribution and continuity of these structures within basins and along prospective sand fairways remains highly uncertain.

Conclusions

Submarine sediments can remobilize in different ways, including downslope mass wasting, injection caused by catastrophic release of pore fluids and overturn caused by gravitational settling. In all these cases, remobilization can happen long after the formation of the original deposit. However, it can also be caused by turbidity currents and be concurrent with deposition of turbidite sands. Recognition and interpretation of synkinematic growth strata is critical for understanding the

relationship between deformation, deposition and inferred flow processes in turbidity currents. Outcrop studies reported here show deformation beneath sandy turbidites that we interpret as being caused by the partitioning of shear strain into the substrate of turbidity currents during their emplacement. The case studies we use to illustrate our discussion are by no means unusual or rare: in our experience, kinematic boundary layers are commonly preserved in turbidite successions globally and through geological time. In this paper a framework for characterizing deformation of the syndepositional seabed caused by overriding turbidity currents has been presented. Such frameworks are useful for the interpretation of turbidite deposits, the distribution and continuity of bed heterogeneities, and the deduction of the dynamics of the turbidity currents that created them.

Acknowledgements and Funding

Scientific editing by Stuart Jones

References

Allen, J.R.L. 1984. *Sedimentary Structures, Their Character and Physical Basis*, unabridged one-volume edition. Elsevier, Amsterdam.

Amore, F.O., Bonardi, G., Ciampo, G., De Capoa, P., Perrone, V. & Sgrosso, I. 1988. Relations between the 'internal Flysch' and Apennine domains: A reinterpretation of the Pollica, San Mauro and Albidona Formations in the intra-Miocenic evolution of the external zones of the Apennines. *Memorie della Società Geologica d'Italia*, **41**, 285–297 [in Italian].

Baas, J.H., Best, J.L. & Peakall, J. 2011. Depositional processes, bedform development and hybrid bed formation in rapidly decelerated cohesive (mud–sand) sediment flows. *Sedimentology*, **58**, 1953–1987.

Baas, J.H., Manica, R., Puhl, E., Verhagen, I. & Borges, A.L.O. 2014. Processes and products of turbidity currents entering soft muddy substrates. *Geology*, **42**, 371–374.

Balance, P.F. 1974. An inter-arc flysch basin in northern New Zealand: Waitemata Group (upper Oligocene to Lower Miocene). *Journal of Geology*, **82**, 439–471.

Barker, S.P., Haughton, P.D.W., McCaffrey, W.D., Archer, S.G. & Hakes, W. 2008. Development of rheological heterogeneity in clay-rich high-density turbidity currents: Aptian Britannia Sandstone Member, UK Continental Shelf. *Journal of Sedimentary Research*, **78**, 45–68.

Bouma, A.H. 1962. *Sedimentology of some Flysch Deposits*. Elsevier, Amsterdam.

Branney, M.J. & Kokelaar, P. 1992. A reappraisal of ignimbrite emplacement: Progressive aggradation and changes from particulate to non-particulate flow during emplacement of high-grade ignimbrite. *Bulletin of Volcanology*, **54**, 504–520.

Brun, J.-P. & Fort, X. 2004. Compressional salt tectonics (Angolan margin). *Tectonophysics*, **382**, 129–150.

Butler, R.W.H. & Tavarnelli, E. 2006. The structure and kinematics of substrate entrainment into high concentration sandy turbidites: A field example from the Gorgoglione 'flysch' of southern Italy. *Sedimentology*, **53**, 655–670.

Cartigny, M.J.B., Eggenhuisen, J.T., Hansen, E.W.M. & Postma, G. 2013. Concentration-dependent flow stratification in experimental high-density turbidity currents and their relevance to turbidite facies models. *Journal of Sedimentary Research*, **83**, 1047–1065.

Cavuoto, G., Martelli, L., Nardi, G. & Valenti, G. 2004. Depositional systems and architecture of Oligo-Miocene turbidite successions in Cilento (southern Apennines). *GeoActa*, **3**, 129–147.

Clark, J.D. & Stanbrook, D.A. 2001. Formation of large-scale shear structures during deposition of high-density turbidity currents. *In*: McCaffrey, W.D., Kneller, B.C. & Peakall, J. (eds) *Particulate Gravity Currents*. International Association of Sedimentologists, Special Publications, **31**, 219–232.

Collinson, J. 1994. Sedimentary deformation structures. *In*: Maltman, A. (ed.) *The Geological Deformation of Sediments*. Chapman & Hall, London, 95–125.

Cornamusini, G., Elter, F.M. & Sandrelli, F. 2002. The Corsica–Sardinia Massif as source area for the early northern Apennines foredeep system: Evidence from debris flows in the 'Macigno costiero' (Late Oligocene, Italy). *International Journal of Earth Sciences*, **91**, 280–290.

Eggenhuisen, J.T., McCaffrey, W.D., Haughton, P.D.W. & Butler, R.W.H. 2010*a*. Shallow erosion beneath turbidity currents and its impact on the architectural development of turbidite sheet systems. *Sedimentology*, **57**, 1365–1391.

Eggenhuisen, J.T., McCaffrey, W.D., Haughton, P.D.W., Butler, R.W.H., Moore, I., Jarvie, A. & Hakes, W.G. 2010*b*. Reconstructing large-scale remobilisation of deep-water deposits and its impact on sand-body architecture from cored wells: The Lower Cretaceous Britannia Sandstone Formation, UK North Sea. *Marine and Petroleum Geology*, **27**, 1595–1615.

Fossen, H., Schultz, R.A., Shipton, Z.K. & Mair, K. 2007. Deformation bands in sandstone: A review. *Journal of the Geological Society, London*, **164**, 755–769, http://dx.doi.org/10.1144/0016-76492006-036.

Garnham, P.J. & Tucker, O.D. 2012. The Longannet to Goldeneye Project: Challenges in developing an end-to-end CCS scheme. Carbon Management Technology Conference, Orlando, Florida, 7–9 February, 151716, http://dx.doi.org/10.7122/151716-MS.

Hanmer, S. & Passchier, C. 1991. *Shear Sense Indicators—A Review*. Geological Survey of Canada, Paper, **90-17**.

Hanna, M.A. 1926. Geology of the La Jolla quadrangle, California. *Bulletin of the University of California, Department of Geological Sciences*, **16**, 87–246.

Haughton, P., Davis, C., McCaffrey, W.D. & Barker, S. 2009. Hybrid sediment gravity flow deposits—classification, origin and significance. *Marine and Petroleum Geology*, **26**, 1900–1918.

Joseph, P. & Lomas, S.A. (eds) 2004. *Deep-Water Sedimentation in the Alpine Basin of SE France: New Perspectives on the Grès d'Annot and Related Systems*. Geological Society, London, Special Publications, **221**.

Kelling, G. & Walton, E.K. 1957. Lode-cast structures: Their relationship to upper-surface structures and their mode of formation. *Geological Magazine*, **94**, 481–490.

Kneller, B. 1995. Beyond the turbidite paradigm: Physical models for deposition of turbidites and their implications for reservoir prediction. *In*: Hartley, A.J. & Prosser, D.J. (eds) *Characterization of Deep Marine Clastic Systems*. Geological Society, London, Special Publications, **94**, 31–49, http://dx.doi.org/10.1144/GSL.SP.1995.094.01.04.

Kneller, B. & Branney, M. 1995. Sustained high-density turbidity currents and the deposition of thick massive sands. *Sedimentology*, **42**, 607–616.

Kneller, B. & Buckee, C. 2000. The structure and fluid mechanics of turbidity currents: A review of some recent studies and their geological implications. *Sedimentology*, **47**, 62–94.

Kneller, B., Edwards, D., McCaffrey, W.D. & Moore, R. 1991. Oblique reflection of turbidity currents. *Geology*, **14**, 250–252.

Kobberger, G. & Schmincke, H.-U. 1999. Deposition of rheomorphic ignimbrite D (Morgàn Formation), Gran Canaria, Canary Islands, Spain. *Bulletin of Volcanology*, **60**, 465–485.

Lowe, D.R. & Guy, M. 2000. Slurry-flow deposits in the Britannia Formation (Lower Cretaceous), North Sea: A new perspective on the turbidity current and debris flow problem. *Sedimentology*, **47**, 31–70.

Lowe, D.R., Guy, M. & Palfrey, A. 2003. Facies of slurry-flow deposits, Britannia Formation (Lower Cretaceous), North Sea: Implications for flow evolution and deposit geometry). *Sedimentology*, **50**, 45–80.

Matsumoto, D., Naruse, H., Fujino, S., Surphawajruksakul, A., Jarupongsakul, T., Sakakura, N. & Murayama, M. 2008. Truncated flame structures within a deposit of the Indian Ocean Tsunami: Evidence of syn-sedimentary deformation. *Sedimentology*, **55**, 1559–1570.

McClelland, H.L.O., Woodcock, N.H. & Gladstone, C. 2011. Eye and sheath fold in turbidite convolute lamination: Aberystwyth Grits Group, Wales. *Journal of Structural Geology*, **33**, 1140–1147.

Mulder, T. & Cochonat, P. 1996. Classification of offshore mass movements. *Journal of Sedimentary Research*, **66**, 43–57.

Mutti, E. 1992. *Turbidite Sandstones*. AGIP–Istituto di Geologia, Universita di Parma, Parma.

Pinnock, S.J. & Clitheroe, A.R.J. 1997. The Captain Field, UK North Sea; appraisal and development of a viscous oil accumulation. *Petroleum Geoscience*, **3**, 305–312.

Postma, G., Cartigny, M. & Kleverlaan, K. 2009. Structureless, coarse-tail graded Bouma Ta formed by internal hydraulic jump of the turbidity current? *Sedimentary Geology*, **219**, 1–6.

Røe, S.L. & Hermansen, M. 2006. New aspects of deformed cross-strata in fluvial sandstones: Examples from Neoproterozoic formations in northern Norway. *Sedimentary Geology*, **186**, 283–293.

Ross, J.A., Peakall, J. & Keevil, G.M. 2013. Subaqueous sand extrusion dynamics. *Journal of the Geological Society, London*, **170**, 593–602, http://dx.doi.org/10.1144/jgs2012-124.

Sovilla, B., Margreth, S. & Bartelt, P. 2007. On snow entrainment in avalanche dynamics calculations. *Cold Regions Science and Technology*, **47**, 69–79.

Sparks, R.S.J., Gardeweg, M.C., Calder, E.S. & Matthews, S.J. 1997. Erosion by pyroclastic flows on Lascar Volcano, Chile. *Bulletin of Volcanology*, **58**, 557–565.

Talling, P.J., Masson, D.G., Sumner, E.J. & Malgesini, G. 2012. Subaqueous density flows: Depositional processes and deposit types. *Sedimentology*, **59**, 1937–2003.

Valente, A., Slaczka, A. & Cavuoto, G. 2014. Soft-sediment deformation structures in seismically affected deep-sea Miocene turbidites. *Geologos*, **20**, 67–78.

Verhagen, I.T.E., Baas, J.H., Davies, A.G., Jacinto, R.S. & McCaffrey, W.D. 2013. A first classification scheme of flow-bed interaction for clay-laden density currents and soft substrates. *Ocean Dynamics*, **63**, 1–13.

Vinnels, J.S., Butler, R.W.H., McCaffrey, W.D. & Lickorish, W.H. 2010. Sediment distribution and architecture around a bathymetrically complex basin: Eastern Champsaur Basin, SE France. *Journal of Sedimentary Research*, **80**, 216–235.

Williams, G.D. 1993. Tectonics and seismic sequence stratigraphy: An introduction. *In*: Williams, G.D. & Dobb, A. (eds) *Tectonics and Seismic Sequence Stratigraphy*. Geological Society, London, Special Publications, **71**, 1–13, http://dx.doi.org/10.1144/GSL.SP.1993.071.01.01.